INFLUENCE OF APPLICATION OF HOTTEL'S ZONAL MODEL AND SIX-FLUX MODEL OF THERMAL RADIATION ON NUMERICAL SIMULATIONS RESULTS OF PULVERIZED COAL FIRED FURNACE

by

Nenad D. CRNOMARKOVIĆ [a*]*, Miroslav A. SIJERČIĆ* [a]*, Srdjan V. BELOŠEVIĆ* [a]*,*
Dragan R. TUCAKOVIĆ [b]*, and Titoslav V. ŽIVANOVIĆ* [b]

[a] Laboratory for Thermal Engineering and Energy, Vinča Institute of Nuclear Scienes,
University of Belgrade, Belgrade, Serbia
[b] Thermal Engineering Department, Faculty of Mechanical Engineering,
University of Belgrade, Belgrade, Serbia

Difference of results of numerical simulation of pulverized coal fired furnace when mathematical models contain various radiation models has been described in the paper. Two sets of numerical simulations of pulverized coal fired furnace of 210 MW$_e$ power boiler have been performed. One numerical simulation has contained Hottel's zonal model, whereas the other numerical simulation has contained six-flux model. Other details of numerical simulations have been identical. The influence of radiation models has been examined through comparison of selected variables (gas-phase temperature, oxygen concentration, and absorbed radiative heat rate of surface zones of rear and right furnace walls), selected global parameters of furnace operation (total absorbed heat rate by all furnace walls and furnace exit gas-phase temperature). Computation time has been compared as well. Spatially distributed variables have been compared through maximal local differences and mean differences. Maximal local difference of gas-phase temperature has been 8.44%. Maximal local difference of absorbed radiative heat rate of the surface zones has been almost 80.0%. Difference of global parameters of furnace operation has been expressed in percents of value obtained by mathematical model containing Hottel's zonal model and has not been bigger than 7.0%. Computation time for calculation of 1000 iterations has been approximately the same. Comparison with other radiation models is necessary for assessment of differences.

Key words: *numerical simulation, pulverized coal, thermal radiation, six-flux model, Hottel's zonal model*

Introduction

In all high-temperature processes, radiation is dominant mode of heat transfer [1]. In contemporary 3-D mathematical models of combustion systems, the following models of thermal radiation are usually used: six-flux model (SFM), discrete ordinates model (DOM), spherical harmonics model (SHM), discrete transfer model (DTM), Monte Carlo model

---

* Corresponding author; e-mail: ncrni@vinca.rs

(MCM), and Hottel's zonal model (HZM) [2-4]. One of the main characteristics of the radiation model is its accuracy of determination of radiative energy source term and radiative wall fluxes.

Accuracy of radiation models were investigated using benchmark tests in 3-D geometry [5-7]. Benchmark tests were used to prove accuracy of the radiation models [8-10] and of their improvements [11, 12]. Some of the comparisons were based on known (*i. e.*, fixed) temperatures and radiative properties [8, 12]. Radiative energy source term and radiative wall fluxes were determined using gray [12] or non-gray [8] radiative properties. In other type of comparison, temperatures and radiative wall fluxes were calculated using known non-radiative energy source term and radiative properties [9-11]. In all types of comparisons, exact values of radiative energy source term and radiative wall fluxes were obtained from exact solution of radiative transfer equation [5] or using HZM [6] or MCM [7].

On the basis of studies on accuracy of radiation models [2-11], all mentioned radiation models can be divided into three groups. HZM and MCM are the most accurate radiation models. DOM, SHM, and DTM belong to the second group of models, whereas the third group of models comprises multiflux models, to which SFM belongs.

Choice of radiation models used in mathematical model of a furnace influences results of numerical simulation. Objective of this paper is to investigate differences of numerical simulation results of pulverized coal fired furnace when mathematical models contain different radiation models. For a chosen pulverized coal fired furnace, two identical comprehensive mathematical models with exception of radiation models have been formed. One mathematical model has contained HZM, whereas the other one has contained SFM. HZM have been chosen as a model that belongs to the group of the most accurate models, and SFM has been chosen as a model that belongs to the group of the modest accurate models.

A furnace of 210 MW_e steam boiler has been chosen for investigation. Detail description of the furnace geometry, operating conditions, and coal properties were already given [13]. Here, the main characteristics are briefly described. Horizontal cross-section of the furnace is 13.5×15.5 m, whereas the height of the furnace is 34.0 m. Because of the furnace hopper (in the lower part of the furnace) and furnace nose (in the upper part of the furnace), furnace volume and surface area of the furnace walls are $V_{fur} = 5669$ m^3 and $A_w = 1934$ m^2, respectively. The furnace is tangentially fired by Kolubara lignite. Coal proximate analysis (as received): moisture 52.67%, ash 11.23%, volatile 21.46%, fixed carbon 14.64%, lower heating value $7.816 \cdot 10^3$ kJ/kg. Coal ultimate analysis (as received): carbon 22.70, hydrogen 2.13, oxygen 10.39, nitrogen 0.50, and sulfur 0.38. Moisture content of pulverized coal, after milling and drying of the raw coal in the coal mill, is reduced to 14.0%.

Description of mathematical models

The present study has been performed by means of in-house developed software. Mathematical model comprises three submodels: turbulence submodel, radiation submodel, and combustion submodel. Turbulence and combustion submodels were already described [13, 14]. Here, only radiation models are described.

HZM of thermal radiation

The HZM of thermal radiation was developed by Hottel *et al.* [15] and by Hottel *et al.* [16]. Model is based on division of furnace volume into *M* isothermal volume zones g_i

and furnace walls into N isothermal surface zones s_i. For each pair of zones, direct exchange areas and total exchange areas are determined. Direct exchange area of two zones represents part of emitted radiation from one zone that is absorbed and scattered in the other zone after travelling by direct route in black-walled enclosure. Total exchange areas take into account radiative exchange between zones by all possible routes and multiple reflection of radiation at the furnace walls.

Total exchange areas are usually used to find radiative energy source term through net radiative absorption. Net radiative absorption of the volume zone g_i is a difference of absorbed radiative heat rate and energy loss by emission of radiation [1]:

$$Q_{\text{net},i} = \sum_{m=1}^{M} \overline{G_m G_i} E_{\text{b},g_m} + \sum_{n=1}^{N} \overline{G_i S_n} E_{\text{b},s_n} - 4K_a V_i E_{\text{b},g_i}, \quad i = 1,...,M \tag{1}$$

where $K_a = K_{a,p} + K_{a,g}$ is the absorption coefficient of the medium and index i is the number of the volume zone.

Radiative energy source term of the volume zone g_i is obtained dividing net radiative absorption by the volume of the zone:

$$q_i''' = \frac{Q_{\text{net},i}}{V_i}, \quad i = 1,...,M \tag{2}$$

Absorbed radiative heat rate of the surface zone s_i is a sum of absorbed radiative heat rates due to emission of radiation from all zones:

$$Q_{\text{a},i} = \sum_{m=1}^{M} \overline{G_m S_i} E_{\text{b},g_m} + \sum_{n=1}^{N} \overline{S_n S_i} E_{\text{b},s_n}, \quad i = 1,...,N \tag{3}$$

where index i is the number of the surface zone. Incident wall flux of the surface zone s_i is determined on the basis of absorbed radiative heat rate:

$$q_{i,\text{inc}} = \frac{Q_{\text{a},i}}{\varepsilon_i A_i}, \quad i = 1,...,N \tag{4}$$

Radiative heat exchange among zones is calculated using algebraic summation. Accuracy of the HZM is based on accuracy of determination of total exchange areas. Various methods were developed for determination and improvement of total exchange areas [17, 18].

SFM of thermal radiation

SFM of thermal radiation, developed by Chu *et al.* [19], was formed for 1-D plane parallel medium. Varma [20] formed equations of the model for cylindrical furnaces in the form of six first-order differential equations, which could be reduced to four equations in the conditions of axial symmetry. Smoot *et al.* [21] transformed the set of four first-order equations to set of two second-order differential equations using approach by Gosman *et al.* [22]. For calculation of radiative heat exchange in 3-D rectangular geometry, Miller *et al.* [23] developed equations of the model in the form of a set of three second-order differential equations.

SFM is based on division of solid angle into six subdivisions, over which radiation intensity is considered isotropic. After integration of radiation intensities over solid angle

274

Crnomarković, N. D., *et al.*: Influence of Application of Hottel's Zonal Model and …
THERMAL SCIENCE, Year 2012, Vol. 16, No. 1, pp. 271-282

subdivisions, radiation fluxes in positive (I_x^+, I_y^+, and I_z^+) and negative (I_x^-, I_y^-, and I_z^-) direction of coordinate axes are obtained. From radiative heat balance over elementary volume, six first-order differential equations of the radiative fluxes are obtained. Six first-order differential equation are reduced to three second-order differential equations using definition of total radiation fluxes ($F_x = I_x^+ + I_x^-$, $F_y = I_y^+ + I_y^-$, and $F_z = I_z^+ + I_z^-$).

Equations of total radiation fluxes are written in the following form:

$$\frac{1}{K_t}\frac{\partial}{\partial x}\left(\Gamma\frac{\partial F_x}{\partial x}\right) = -(1-\omega f - \omega b)F_x + 2\omega s(F_y + F_z) + (1-\omega)\frac{I_b}{3} \tag{5a}$$

$$\frac{1}{K_t}\frac{\partial}{\partial y}\left(\Gamma\frac{\partial F_y}{\partial y}\right) = -(1-\omega f - \omega b)F_y + 2\omega s(F_x + F_z) + (1-\omega)\frac{I_b}{3} \tag{5b}$$

$$\frac{1}{K_t}\frac{\partial}{\partial z}\left(\Gamma\frac{\partial F_z}{\partial z}\right) = -(1-\omega f - \omega b)F_z + 2\omega s(F_y + F_x) + (1-\omega)\frac{I_b}{3} \tag{5c}$$

where $K_t = K_a + K_s$ is total extinction coefficient of medium. $\Gamma = -1/K_t[1 - \omega(f - b)]$ – the coefficient of radiation diffusion, $\omega = K_s/K_t$ – the scattering albedo, and I_b – the raditive flux emitted by elementary volume along all directions. Coefficients f, b, and s are scattering fractions, which describe what fraction of scattered radiation is directed forward, backward, and sideways. They satisfy relation $f + b + 4s = 1$. For isotropic scattering $f = b = s = 1/6$.

Radiative energy source term of the i-th control volume is evaluated from following relation [21]:

$$q_i''' = K_{a,g}(F_{x,i} + F_{y,i} + F_{z,i} - I_{b,i}) \tag{6}$$

Incident wall radiation flux of the surface zone is obtained approximately:

$$q_{i,\text{inc}} \approx \frac{F_{n,i} - k\varepsilon\sigma T_w^4}{1 + k\rho} \tag{7}$$

where F_n is total radiation flux in direction of normal to the wall (subscript n stands for x, y, or z) and $k = 1/3$ is the number that takes into account division of the solid angle. Surface zone in SFM is a boundary surface of the control volume next to the wall that is shared by the control volume and the wall.

Equations of total radiation fluxes are discretized using method of control volumes [24]. Equations 5(a-c) are solved using the same method that is applied for solution of gas-phase differential equations. That is an important charcteristic of the SFM, because it reduced overall complexity of mathematical model.

Radiative and thermodynamic properties

Radiative properties of the pulverized coal flame have been determined using gray radiative properties. Pulverized coal flame is a two-phase medium, composed of gaseous products of combustion and cloud of particles. Absorption coefficient of the gas-phase of the medium has been determined using single gray gas model [8]. Pulverized coal flame contains various particles: coal particles, char particles, soot particles, and flyash particles [1]. Seeker

Crnomarković, N. D., *et al.*: Influence of Application of Hottel's Zonal Model and …
THERMAL SCIENCE, Year 2012, Vol. 16, No. 1, pp. 271-282

275

et al. [25] showed that soot particles in pulverized coal flame existed in negligible amounts. Influence of coal, char, and flyash particles on radiative properties of pulverized coal flame was described by Blokh [26]. Coal particles exist only in the vicinity of the burner. Char particles exist only in the active combustion zone, which is not very extensive. Flyash particles are present in the whole furnace volume and exert the strongest influence on radiative properties of pulverized coal flame.

Pulverized coal flame is an inhomogeneous medium. Radiative properties of the dispersed phase depend on particle size distribution, particle number concentration, and complex index of refraction of particles [26]. All these parameters could not be accurately determined, so that approximations have been necessary. Also, efficient methods for appplication of the HZM have been developed only for homogeneous medium. Because of that, radiative properties of the medium in both mathematical models have been determined for homogeneous medium.

Method of determination of radiative properties was already described [27]. Values of radiative properties are given in tab. 1.

Total hemispherical emissivity $\varepsilon = 0.8$ of the furnace walls is determined for ash deposits at supposed wall temperature $T_w = 615.0$ K [26]. The gas-phase thermo-dynamic properties have been determined using equation of state, semi-empirical relations, and regressions [24].

Table 1. Radiative properties of medium

Absorption coefficient of the gas-phase of medium [m^{-1}]	0.076
Absorption coefficient of the cloud of particles [m^{-1}]	0.070
Scattering coefficient of the cloud of particles [m^{-1}]	0.127
Total extinction coefficient [m^{-1}]	0.273
Scattering albedo [–]	0.465

Results

Results are presented through proof of grid independence, verification of mathematical models, and comparison of results of numerical simulations.

Grid independence and verification of mathematical models

Proof of grid independence and verification of mathematical models have been shown using numerical simulation containing HZM of thermal radiation.

A 3-D staggered, block-structured, and orthogonal numerical grid has been used in numerical simulation containing HZM of thermal radiation. Radiative heat exchange has been solved on coarse numerical grid ($40 \times 14 \times 16$), which has been composed of cubical volume zones. Edge dimension of the volume zone has been $B = 1.0$ m. Surface zones have been squares of the same edge dimension. Because of the contraction of the furnace cross-section in the lower part (furnace hopper) and in the upper part (furnace nose), total number of the volume and surface zones have been $M = 7956$ and $N = 2712$, respectively.

To evaluate influence of numerical grid on results, three fine meshes have been formed: $162 \times 44 \times 50 = 356,400$ nodes, $162 \times 58 \times 66 = 620,136$ nodes, and $162 \times 72 \times 82 = 956,448$ nodes. Fine numerical grids have been obtained dividing each volume zones into equal number of cubical control volumes. All fine numerical grids have been uniform. Comparison of results of numerical simulations for different numerical grids has indicated that grid-independent solution is obtained using numerical grid having 620,136 nodes.

Verification of the mathematical model containing HZM of thermal radiation has been done through comparison of numerical simulation results with results of measurements. Available results of measurements are incident radiative fluxes and flame temperatures measured by optical pyrometer along the left furnace wall at the level of 22.3 m from the furnace bottom [28]. Comparison is shown in tab. 2.

Table 2. Verification of mathematical model

Distance from front wall [m]	Incident flux [Wm^{-2}]		Difference [%]	Temperature [K]		Difference [%]
	Measured	Predicted		Measured	Predicted	
2.0	$1.65 \cdot 10^5$	$1.44 \cdot 10^5$	12.7	1383.0	1426.0	3.1
6.0	$2.05 \cdot 10^5$	$1.89 \cdot 10^5$	7.8	1443.0	1525.0	5.7
12.0	$1.84 \cdot 10^5$	$1.62 \cdot 10^5$	11.9	1433.0	1328.0	7.3

Difference of the results obtained by measurement and by numerical simulation has been expressed in percents of measured values. Results presented in tab. 2 show acceptable agreement between measurement and numerical simulation.

Comparison of results of numerical simulations

In this work, mathematical models have been used for determination of physical variables and for determination of global parameters of furnace operation.

Physical variables that have been chosen for comparison are gas-phase temperature, oxygen mass concentration, and absorbed radiative heat rate of surface zones of rear and right furnace walls. Analyses of differences have been carried out using local difference:

$$\delta\eta_i = \frac{\left|\eta_{\mathrm{hzm},i} - \eta_{\mathrm{sfm},i}\right|}{\eta_{\mathrm{hzm},i}}100 \tag{8}$$

where η stands for all analyzed variables. Subscripts hzm and sfm show that variable has been determined by mathematical model containing HZM or SFM, respectively. Subscript i designates control volume for gas-phase temperature and oxygen mass concentration, or surface zone for absorbed radiative heat rate of surface zones.

Gas-phase temperatures and local differences of the gas-phase temperatures are shown in figs. 1(a-c) and 2(a-c). Absorbed radiative heat rates of rear and right furnace walls and their local differences are shown in figs. 3(a-c) and 4(a-c). Obtained changes of gas-phase temperature along the furnace height and absorbed heat rate along the height of furnace wall are typical for tangentially fired furnaces [29]. Dashed lines at figs 1 and 2 mark the position of the furnace exit plane.

Maximal local difference represents the entire interval of difference of analyzed variable. Maximal local differences of analyzed variables have been following: 8.44% for gas-phase temperature, 19.60% for oxygen mass concentration, 61.48% for absorbed radiative heat rate of surface zone of rear furnace wall, and 79.40% for absorbed radiative heat rate of surface zone of right furnace wall.
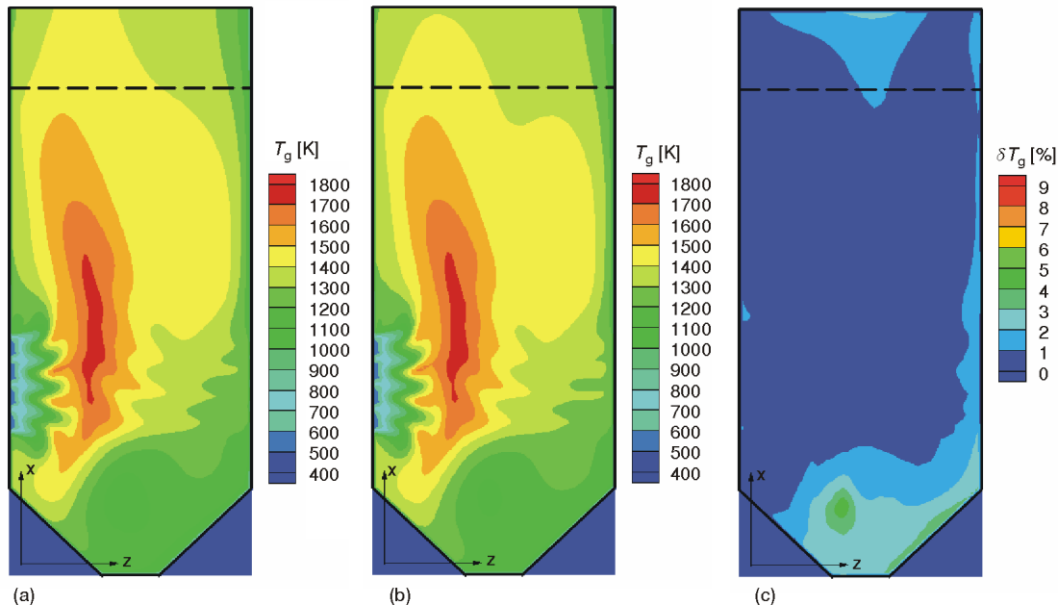
Figure 1. Gas-phase temperature at middle plane *y* = const.: (a) mathematical model containing HZM, (b) mathematical model containing SFM, (c) local difference (color image see on our web site)
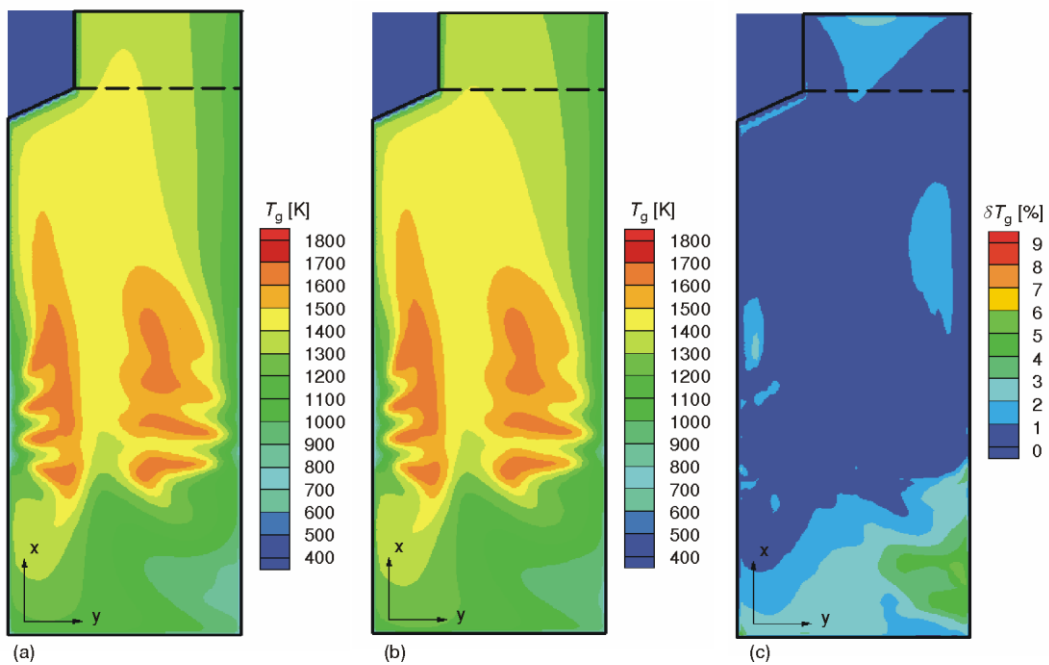

Figure 2. Gas-phase temperature at middle plane *z* = const.: (a) mathematical model containing HZM, (b) mathematical model containing SFM, (c) local difference (color image see on our web site)

278

Crnomarković, N. D., *et al.*: Influence of Application of Hottel's Zonal Model and …
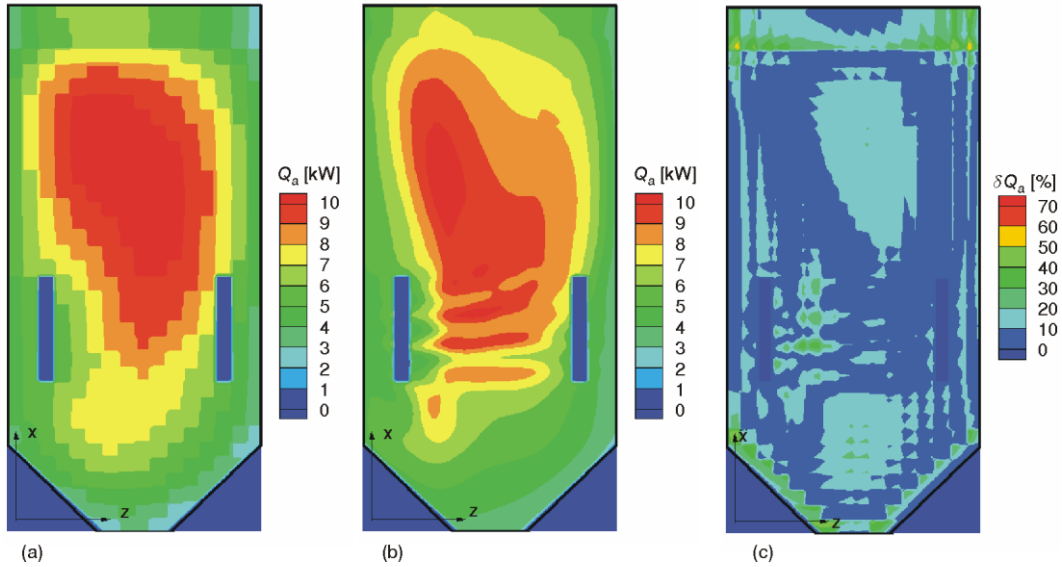THERMAL SCIENCE, Year 2012, Vol. 16, No. 1, pp. 271-282

Figre 3. Absorbed radiative heat rate of rear furnace wall: (a) mathematical model containing HZM, (b) mathematical model containing SFM, (c) local difference (color image see on our web site)
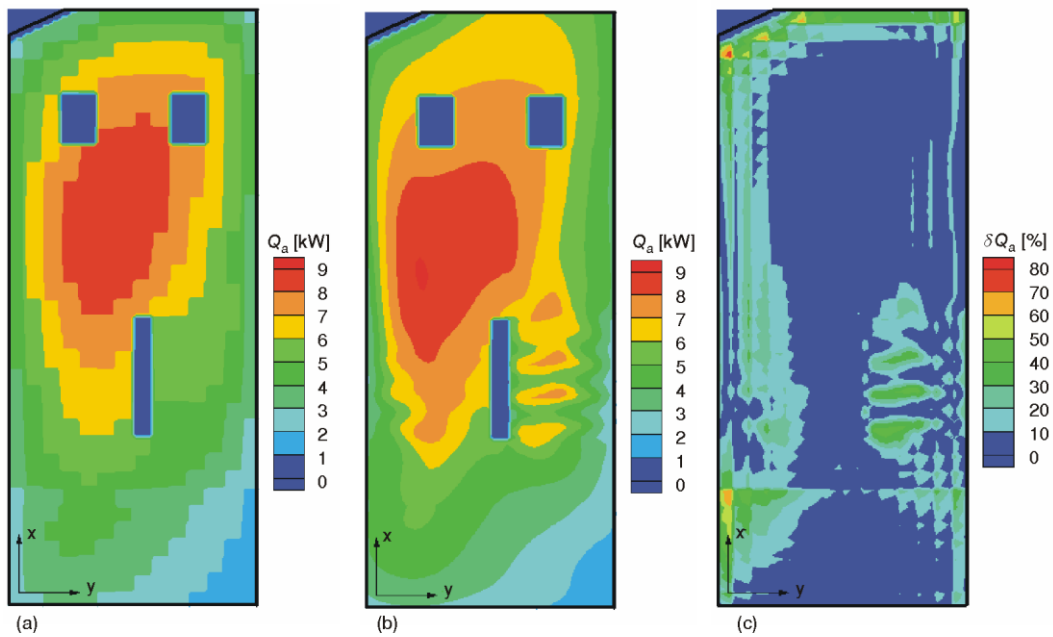

Figure 4. Absorbed radiative heat rate of right furnace wall: (a) mathematical model containing HZM, (b) mathematical model containing SFM, (c) local difference (color image see on our web site)

Mean differences of gas-phase temperature and oxygen mass concentration have been calculated summing local differences multiplied by weighting factors that represent relative size of control volumes:

$$\Delta \Phi = \sum_i \delta \Phi_i \frac{V_i}{\sum_i V_i} \tag{9}$$

where subscript i designates control volumes. Mean difference of the gas-phase variable represents grouping of the local differences between minimal (0.0%) and maximal local difference. Mean difference of gas-phase temperature has been 0.88%, whereas mean difference of oxygen mass concentration has been 0.69%. Small values of mean differences of analyzed gas-phase variables show that their local differences of the most control volumes are close to the minimal value of local difference. That is also evident from the figs. 1(c) and 2(c).

Mean differences of absorbed radiative heat rate of surface zones of chosen furnace wall have been calculated summing local differences multiplied by weighting factors that represent contribution of local absorbed radiative heat rate to total absorbed radiative heat rate of the furnace wall:

$$\Delta Q_a = \sum_i \delta Q_{a,i} \frac{Q_{a,\mathrm{hzm},i}}{\sum_i Q_{a,\mathrm{hzm},i}} \tag{10}$$

where subscript i designates surface zones. Mean differences of the absorbed radiative heat rate of surface zones have been 9.69% for rear furnace wall and 10.22% for right furnace wall. Differences of absorbed radiative heat rate are consequences of both different gas-phase temperatures and different method of calculation. To find which one of them has bigger influence, absorbed radiative heat rates have been calculated using the method based on HZM and gas-phase temperatures obtained by both mathematical models. Local difference and mean difference have been calculated using eqs. (8) and (10). Indexes hzm and sfm in this case indicate absorbed heat rate obtained using gas-phase temperatures from mathematical model containing HZM or SFM, respectively. Maximal local difference has been 11.60% (for both walls), and mean differences have been 2.11% for rear furnace wall and 3.32% for right furnace wall. This analysis has shown that main reason for different values of absorbed radiative heat rates of surface zones is different method of calculation.

Selected analyzed global parameters of furnace operation have been total absorbed radiative heat rate by each furnace wall, total absorbed radiative heat rate by all furnace walls, and furnace exit gas-phase temperature (FEGT). These parameters are given in tab. 3.

Table 3. Selected global parameters of furnace operation and computation time

Total absorbed radiative heat rate [MW]	Mathematical model containing HZM	Mathematical model containing SFM	Difference [%]
Rear furnace wall	57.27	55.88	2.42
Right furnace wall	39.51	42.00	6.30
Front furnace wall	41.96	44.58	6.24
Left furnace wall	46.28	46.60	0.007
All furnace walls	185.02	189.06	2.18
FEGT [K]	1392.6	1317.7	5.4
Computation time[a] [h]	≈30	≈30	–

[a] For calculation of 1000 iterations

280

Crnomarković, N. D., *et al.*: Influence of Application of Hottel's Zonal Model and ...
THERMAL SCIENCE, Year 2012, Vol. 16, No. 1, pp. 271-282

Differences presented in tab. 3 have been expressed in percents of parameters obtained by mathematical model containing HZM. FEGT has been determined as arithmetic mean of all gas-phase temperatures in the furnace exit plane. Differences of total absorbed radiative heat rates by furnace walls have been smaller than differences of absorbed heat rates obtained by eqs. (8) and (10). Obviously, without the absolute difference in eq. (8) some local differences would be positive and some would be negative.

Convergence of numerical solution has been achieved after approximately 2000 iterations. Computation time needed for calculation of 1000 iterations has been included in tab. 3. Computation time depends on involved computer memory. In the case of mathematical model containing SFM, involved computer memory depends on numerical grid. Involved computer memory of a mathematical model containing HZM is even bigger, for computer memory needed for matrices of total exchange areas. In our previous work, numerical grid was composed of $\approx 80,000$ nodes, and computation time needed for 2000 iterations of mathematical model containing HZM was 2 times of that needed for mathematical model containing SFM. For numerical grid composed of 620,136 nodes, computation time has been almost the same for both types of numerical simulations. Involved computer memory has not influenced computation time for such number of nodes.

Conclusions

This investigation has indicated differences of results of the numerical simulations when comprehensive mathematical model contains different radiation models. To further compare differences of results of numerical investigation when comprehensive mathematical model contains various radiation models, radiation models of the second group of accuracy (DOM, SHM, and DTM) should be involved in the study. Comparison of various mathematical models would provide complete insight into influence of radiation models on results of numerical simulation of pulverized coal fired furnaces.

Acknowledgment

Nomenclature

A – surface area, [m^2]
B – zone edge dimension, [m]
b – scattering fraction, [–]
E_b – blackbody emissive power, [Wm^{-2}]
F – total radiation flux, [Wm^{-2}]
f – scattering fraction, [–]
g – volume zone
$\overline{GG}$ – total exchange area for two volume zones, [m^2]
$\overline{GS}$ – total exchange area for volume and surface zone, [m^2]
I – radiation flux, [Wm^{-2}]
I_b – blackbody radiation flux, [Wm^{-2}]

K_a – absorption coefficient, [m^{-1}]
K_s – scattering coefficient, [m^{-1}]
K_t – total extinction coefficient, [m^{-1}]
M – total number of volume zones, [–]
N – total number of surface zones, [–]
Q – radiative heat rate, [W]
q – wall flux, [Wm^{-2}]
q''' – radiative energy source term, [Wm^{-3}]
$\overline{SS}$ – total exchange area for two surface zones, [m^2]
s – surface zone; scattering fraction, [–]
T – temperature, [K]

Crnomarković, N. D., *et al.*: Influence of Application of Hottel's Zonal Model and …
THERMAL SCIENCE, Year 2012, Vol. 16, No. 1, pp. 271-282

281

V – volume, [m^3]

Greek symbols

Γ – coefficient of radiation diffusion, [m]
Φ – general gas-phase variable
Δ – mean difference
δ – local difference
ε – emissivity, [–]
η – general variable
ρ – reflectivity, [–]
σ – Stefan-Boltzmann constant, [Wm^{-2}K^{-4}]
ω – scattering albedo, [–]

Subscripts and superscripts

a   – absorbed
b   – blackbody
fur   – furnace
g   – gas phase
hzm   – Hottel's zonal model

inc   – incident
m – number of the volume zone
n – number of the surface zone
net   – net
p   – dispersed phase
sfm   – six-flux model
w   – wall
x, y, z – co-ordinate axes
+, –   – positive or negative direction of co-ordinate axis

Acronyms

DOM   – discrete ordinate model
DTM   – discrete transfer model
FEGT   – furnace exit gas temperature
HZM   – Hottel's zonal model
MCM   – Monte Carlo model
SFM   – six-flux model
SHM   – spherical harmonics model

References

[1] Modest, M. F., Radiative Heat Transfer, Academic Press, New York, USA, 2003
[2] Viskanta, R., Menguc, M. P., Radiation Heat Transfer in Combustion Systems, *Progress in Energy and Combustion Science, 13* (1987), 2, pp. 97-160
[3] Viskanta, R., Computation of Radiative Transfer in Combustion Systems, *International Journal of Numerical Methods for Heat & Fluid Flow, 18* (2008), 3/4, pp. 415-442
[4] Mishra, S. C., Prasad, M., Radiative Heat Transfer in Participating Media – A Review, *Sadhana, 23* (1998), 2, pp. 213-232
[5] Selcuk, N., Exact Solutions for Radiative Heat Transfer in Box-Shaped Furnaces, *ASME Journal of Heat Transfer, 107* (1985), 3, pp. 648-655
[6] Menguc, M. P., Viskanta, R., Radiative Transfer in Three-Dimensional Rectangular Enclosures Containing Inhomogeneous, Anisotropically Scattering Media, *Journal of Quantitative Spectroscopy & Radiative Transfer, 33* (1985), 6, pp. 533-549
[7] Liu, F., Numerical Solutions of Three-Dimensional Non-Grey Gas Radiative Transfer Using the Statistical Narrow-Band Model, *ASME Journal of Heat Transfer, 121* (1999), 1, pp. 200-203
[8] Coelho, P. J., Numerical Simulation of Radiative Heat Transfer from Non-Gray Gases in Three-Dimensional Enclosures, *Journal of Quantitative Spectroscopy & Radiative Transfer, 74* (2002), 3, pp. 307-328
[9] Wei, X. L., Xu, T. M., Hui, S. E., Three-Dimensional Radiation in Absorbing-Emitting-Scattering Medium Using the Discrete-Ordinates Approximation, *Journal of Thermal Science, 7* (1998), 4, pp. 255-263
[10] Kim, S. H., Huh, K. Y., A New Angular Discretization Scheme of the Finite Volume Method for 3-D Radiative Heat Transfer in Absorbing, Emitting and Anisotropically Scattering Media, *International Journal of Heat and Mass Transfer, 43* (2000), 7, pp. 1233-1242
[11] Selcuk, N., Ayranci, I., The Method of Lines of the Discrete Ordinates Method for Radiative Heat Transfer in Enclosures Containing Scattering Media, *Numerical Heat Transfer, Part B, 43* (2003), 2, pp. 179-201
[12] Selcuk, N., Kirbas, G., The Method of Lines of the Discrete Ordinates Method for Radiative Heat Transfer in Enclosures Containing Scattering Media, *Numerical Heat Transfer, Part B, 37* (2000), 3, pp. 379-392
[13] Belošević, S., *et al.*, Three-Dimensional Modeling of Utility Boiler Pulverized Coal Tangentially Fired Furnace, *International Journal of Heat and Mass Transfer, 49* (2006), 19-20, pp. 3371-3378
[14] Sijerčić, M., Belošević, S., Stefanović, P., Modeling of Pulverized Coal Combustion Stabiliation by Means of Plasma Torches, *Thermal Science, 9* (2005), 2, pp. 57-72

[15] Hottel, H. C., Cohen, E. S., Radiant Heat Exchange in a Gas-Filled Enclosure: Allowance of Nonuniformity of Gas Temperature, *AIChE Journal, 4* (1958), 1, pp. 3-14

[16] Hottel, H. C., Sarofim, A. F., Radiative Transfer, McGraw-Hill, New York, USA, 1967

[17] Rhine, J. M., Tucker, R. J., Modelling of Gas-Fired Furnaces and Boilers, British Gas plc, London, 1991

[18] Mechi, R., *et al*., Extension of the Method to Inhomogenous Non-Gray Semi-Transparent Medium, *Energy, 35* (2010), 1, pp. 1-15

[19] Chu, C. M., Churchill, S. W., Numerical Solution of Problems in Multiple Scattering of Electromagnetic Radiation, *The Journal of Physical Chemistry, 59* (1955), 9, pp. 855-863

[20] Varma, S. A., Radiative Heat Transfer in a Pulverized-Coal Flame, in: Pulverized-Coal Combustion and Gasification, (Eds. L. D. Smoot, D. T. Pratt), Plenum Press, New York, USA, 1979, pp. 83-106

[21] Smoot, L. D., Smith, P. J., Coal Combustion and Gasification, Plenum Press, New York, USA, 1985

[22] Gosman, A. D., Lockwood, F. C., Incorporation of a Flux Model for Radiation Into a Finite-Difference Procedure for Furnace Calculations, *Proceedings*, 14th Symposium (International) on Combustion, Penn., USA, 1972, The Combustion Institute, Pittsburgh, Penn., USA, 1973, pp. 661-670

[23] Miller, F. J., Koenigsdorff, R. W., Thermal Modeling of a Small-Particle Solar Central Receiver, *ASME Journal of Solar Energy Engineering, 122* (2000), 1, pp. 23-29

[24] Sijerčić, M. Mathematical Modelling of Complex Turbulent Transport Processes (in Serbian), Yugoslav Association of Thermal Engineers and VINČA Institute of Nuclear Sciences, Belgrade, 1998

[25] Seeker, W. R., *et al*., The Thermal Decomposition of Pulverized Coal Particles, *Proceedings*, 18th Symposium (International) on Combustion, Waterloo, Ont., Canada, 1980, The Combustion Institute, Pittsburgh, Penn., USA, 1981, pp. 1213-1226

[26] Blokh, A. G., Heat Transfer in Steam Boiler Furnaces, Hemisphere Publishing Corporation, New York, USA, 1988

[27] Crnomarković, N. D., Sijerčić, M. A., Belošević, S. V., Modelling of Radiative Heat Transfer inside the Pulverized Coal Fired Furnace of Power Plant, *Proceedings*, International Symposium Power Plants 2008, Vrnjacka Banja, Serbia, 2008, pp. 1-10

[28] Pavlović, P., Riznić, J., Results of Thermal Measurements in the Furnace of the Power Plant Nikola Tesla No. 2, Report IBK-ITE-313 (in Serbian), Vinča Institute of Nuclear Sciences, Belgrade, 1977

[29] Ivanović, V. B., Reliable Simple Zonal Method of the Furnace Thermal Calculation, *Thermal Science, 9* (2005), 2, pp. 45-55